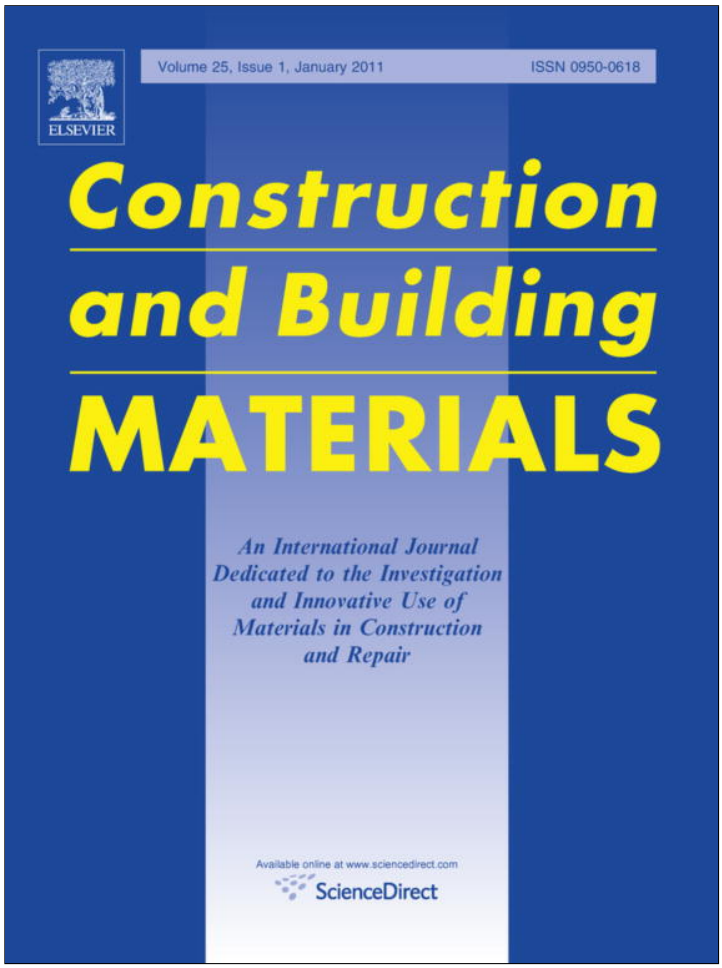

(This is a sample cover image for this issue. The actual cover is not yet available at this time.)

Construction and Building Materials 29 (2012) 56–72

Contents lists available at SciVerse ScienceDirect

Construction and Building Materials

journal homepage: www.elsevier.com/locate/conbuildmat

Experimental and numerical investigation of size effects in FRP-wrapped concrete columns

Hussein M. Elsanadedy *,[1], Yousef A. Al-Salloum, Saleh H. Alsayed, Rizwan A. Iqbal

Specialty Units for Safety & Preservation of Structures, Department of Civil Engineering, King Saud University, P.O. Box 800, Riyadh 11421, Saudi Arabia

ARTICLE INFO

Article history:
Received 11 April 2011
Received in revised form 17 September 2011
Accepted 2 October 2011

Keywords:
Confined concrete
FRP
Size effect
Finite element modeling

ABSTRACT

Some FRP confinement models available in the literature are based on standard cylindrical specimens and others are based on mixed sizes of cylindrical specimens. The accuracy of the latter models is questionable, as it depends on the percentage of increase in strength between unconfined and FRP-confined specimens and on the ratio of strength increase among the different sizes of specimens. The question which can be raised here is: is there a need to introduce a size factor for the test results which are based on non-standard sizes of cylindrical specimens before using them in developing analytical models for FRP-confined concrete? The output of this study answers this important question. Thirty-seven concrete cylinders with three different sizes were experimentally tested. Of these, 13 cylinders were control specimens, to be used as baseline for comparison, whereas the remaining 24 cylinders were wrapped with layers of CFRP jacket. Studied parameters were specimen size and confinement stress ratio. In addition to the experimental investigation, non-linear finite element analysis was also carried out using LS-DYNA software. The predictions of the numerical finite element models were found to agree well with the experimental results of the specimens tested in this study in addition to others selected from the literature. Based on this validation, the effect of specimen size on FRP-confined concrete cylinders was further investigated numerically taking into consideration various confinement ratios and cylinder sizes. The results show that the effect of specimen size on FRP-confined concrete is insignificant.

1. Introduction

During the early 90s, most of the external confinement techniques for columns included increasing the section by either constructing an additional concrete cage or by installing grout-injected steel jackets. Both methods are labor intensive and present difficulties at the site. Presently, fiber-reinforced polymer (FRP) confinement of reinforced concrete columns has been shown to be a very effective technique for structural enhancement. FRP's also present various advantages such as, light weight, high confinement strength, high strength-to-weight ratio, easier installation and maintenance and also durable. FRP-wrapping, prefabricated laminate jacketing and filament winding can substantially enhance the axial compressive strength and ductility of concrete columns due to lateral confinement as demonstrated by numerous investigators, e.g. [1–3]. Studies have also shown that FRP-confined concrete behaves differently from steel-confined concrete [4], so design recommendations developed for steel-confined concrete columns (or cylinders) cannot be applied to FRP-confined columns despite the apparent similarity between these two types of columns or cylinders. Toutanji and Balagurce [5] investigated effectiveness of FRP wrapping for strengthening plain concrete cylinders. Two layers of CFRP or GFRP wrap were applied to the cylinder. They observed 200% and 100% increase in the compressive strength with CFRP and GFRP wraps, respectively. Parvin and Jamwal [6] investigated the behavior of small-scale FRP-wrapped concrete cylinders under uniaxial compressive loading using nonlinear finite element analysis. They considered two parameters for the numerical study: the FRP wrap thickness, and the ply configuration. The finite element analysis results showed substantial increase in the axial compressive strength and ductility of the FRP-confined concrete cylinders as compared to the unconfined ones. The increase in wrap thickness also resulted in enhancement of axial strength and ductility of the concrete cylinders. Berthet et al. [7] presented the results of an experimental investigation concerning the compressive behavior of short concrete columns externally confined by carbon and E-glass FRP jackets. The results showed that external confinement can significantly improve the ultimate strength and ductility of the specimens. Lam and Teng [8] proposed a design-oriented stress–strain model for concrete confined by FRP wraps with fibers only or predominantly in the hoop direction. The model is based on a careful interpretation of existing test data and observations. The predictions of the model

* Corresponding author. Tel.: +966 597938718.
E-mail address: elsanadedy@yahoo.com (H.M. Elsanadedy).
[1] On leave from the Department of Civil Engineering, Helwan University, Cairo, Egypt.

0950-0618/$ - see front matter © 2011 Elsevier Ltd. All rights reserved.
doi:10.1016/j.conbuildmat.2011.10.025

Table 1
Test matrix used in this study.

Specimen designation	Diameter, D (mm)	Height, H (mm)	No. of CFRP layers	Thickness of CFRP jacket, t_j (mm)	Confinement ratio $\left(\rho_j = \frac{4t_j}{D}\right)$	No. of specimens
U-50	50	100	–	–	0	4
U-100	100	200	–	–	0	4
U-150	150	300	–	–	0	5
W1-50	50	100	1	1	0.08	4
W1-100	100	200	1	1	0.04	5
W2-100	100	200	2	2	0.08	4
W1-150	150	300	1	1	0.027	5
W2-150	150	300	2	2	0.053	2
W3-150	150	300	3	3	0.08	4
Total no. of specimens						37

Table 2
Proportions of ingredients used for concrete mix.

Ingredients	Quantity (for 1 m^3)
Cement (type 1)	350 kg
Silica sand	585 kg
Washed sand	195 kg
10 mm aggregate (3/8″)	315 kg
20 mm aggregate (3/4″)	735 kg
Free water	175 kg
Absolute water	3.82
Admixture	0.6% by weight of cement

(a) Control

(b) CFRP-wrapped

Fig. 1. Test specimens.

were found to agree well with test data. Almusallam [9] conducted a comprehensive experimental program which involved 54 plain concrete cylinders with varying compressive strength wrapped with E-glass/epoxy fiber reinforced polymer (GFRP) jackets and subjected to uniaxial compressive loads. The influence of number of composite plies (i.e. composite thickness) and concrete compressive strength on the behavior of the GFRP-confined cylinders was investigated. The results of this study showed that: (i) compressive strength and ductility of the concrete cylinders increases with number of composite layers; and (ii) effect of confinement is substantial for normal strength concrete and marginal for high-strength concrete. A semi-empirical theoretical model was also developed in order to predict stress–strain relationship of GFRP-confined concrete cylinders. The model results showed an excellent agreement with experimental values. Youssef et al. [10] developed a stress–strain model for concrete confined by fiber reinforced polymer (FRP) composites. The model was based on the results of a comprehensive experimental program including large-scale circular, square and rectangular short columns confined by carbon/epoxy and E-glass/epoxy jackets providing a wide range of confinement ratios. Ultimate stress, rupture strain, jacket parameters, and cross-sectional geometry were found to be significant factors affecting the stress–strain behavior of FRP-confined concrete. Such parameters were analyzed statistically based on the experimental data, and equations to theoretically predict these parameters were presented. Experimental results from this study were compared with the proposed semi-empirical model as well as others from the literature. However, most experimental studies to date on the confinement of concrete columns with FRP have been conducted without considering the possible scale factors involved. The behavior of small specimens may be affected by the restraining influence of the end-bearing plates, which can lead to local non-homogeneities that will cause higher standard deviations and produce results that are not representative of larger specimens [11,12]. Most codes provide weighting factors for concrete strengths measured from cylinders having a diameter different than the standard value of 150 mm. Nevertheless, in spite of all these inconveniences, small specimens are widely used since they are more economical, requiring less material, smaller molds, less expensive testing equipment, and limited space for storage. They are also easier to handle, therefore saving time and reducing the risk of damage during handling. Sener et al. [13] studied the size effect on axially loaded reinforced concrete. The test specimens were geometrically similar pin-ended concrete columns of different sizes (in the ratio 1:2:4) giving slenderness ratios of 9.7, 18.0, and 34.7. The columns had square cross sections of sides 50, 100, and 200 mm, and varied in length from 0.14 m to 2.08 m. It was observed that for all slenderness ratios considered in the investigation, the failure loads exhibited a size effect in which the nominal stress at maximum load (failure load divided by cross-sectional area) decreased as the size was increased. This contradicts the

(a) 50-mm cylinders

(b) 100-mm cylinders

(c) 150-mm cylinders

Fig. 2. Instrumented cylinder specimens ready for testing.

(a) Control

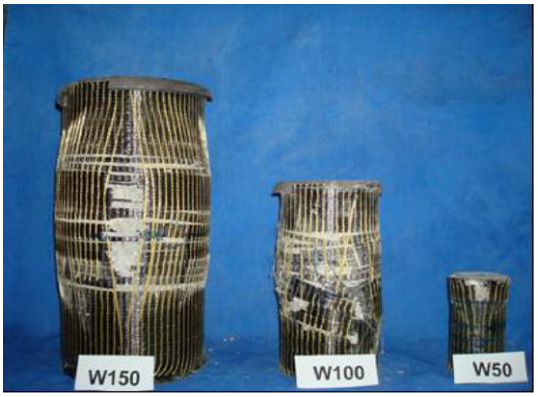

(b) CFRP-wrapped

Fig. 3. Mode of failure of test specimens.

Table 3
Summary of experimental test results.

Specimen designation	Peak axial stress* f'_{cu} (MPa)	$\frac{f'_{cu}}{f'_c}$	$\frac{f'_{cu}}{f'_{co}}$	Peak axial strain* ϵ_{cu} (micro-strain)	$\frac{\epsilon_{cu}}{\epsilon_{co}}$	$\frac{\epsilon_{cu}}{\epsilon_{cuu}}$	Peak lateral strain* (micro-strain)
U-50	53.8	1.31	1.00	3440	1.15	1.00	1316
U-100	49.1	1.19	1.00	3605	1.20	1.00	1138
U-150	41.1	1.00	1.00	3616	1.21	1.00	1172
W1-50	146.2	3.56	2.72	15,625	5.21	4.54	10,479
W1-100	94.5	2.30	1.92	10,907	3.64	3.03	10,323
W2-100	146	3.55	2.97	15,410	5.14	4.27	10,779
W1-150	76.4	1.86	1.86	9445	3.15	2.61	11,807
W2-150	111.5	2.71	2.71	13,353	4.45	3.69	10,071
W3-150	144.2	3.51	3.51	14,852	4.95	4.11	12,151

* Average values of tested specimens.

current design codes, which make no allowance for such size effect, and indicates that the failure is governed by fracture mechanics. Theriault et al. [14] investigated experimentally the influence of slenderness ratio and specimen size on axially loaded FRP-confined concrete columns, and the results have been compared to theoretical models and experimental results gathered from the published literature. Three different specimen diameters and two slenderness (length-to-diameter) ratios, combined with two FRP-confinement materials, were varied as parameters. According to the statistical analysis of the results, it was shown that conventional FRP-confined concrete cylinders can effectively be used to model the axial behavior of short columns. According to the conclusions made in this study, size effects were clearly evident in the small cylinders. However, the validity of the theoretical models developed in this study based on test data from testing small diameter cylinders would be questionable. Masia et al. [15] studied the use of carbon fiber reinforced polymer (CFRP) wrapping to strengthen plain concrete prisms of square cross-section. Increase in axial compressive strength, ductility, and the effect of cross-sectional size were studied. Thirty prisms of three different cross-sectional sizes were tested in this study. It was noticed that the strength and ductility of the prisms was significantly improved. It was also concluded that the effectiveness of the wrap reduced with increasing cross-sectional size. The experimental tests from the study suggested that CFRP wrapping is an effective technique for strengthening and (or) rehabilitating concrete columns.

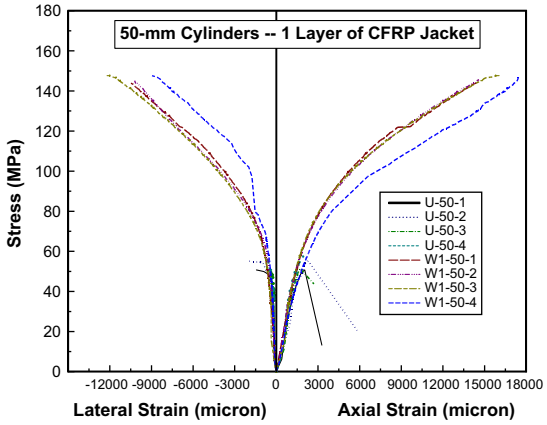

Fig. 4. Stress–strain curves for 50-mm cylinders.

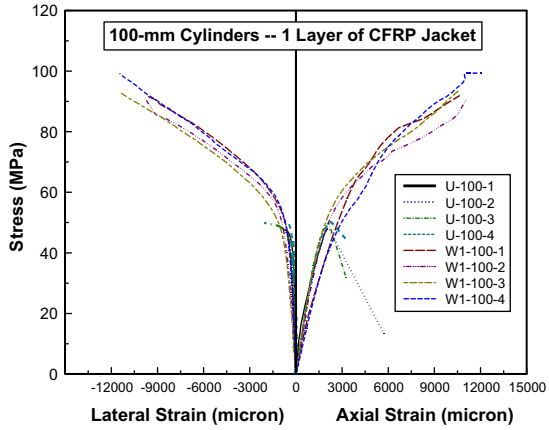

(a) Specimens with 1 layer of CFRP jacket

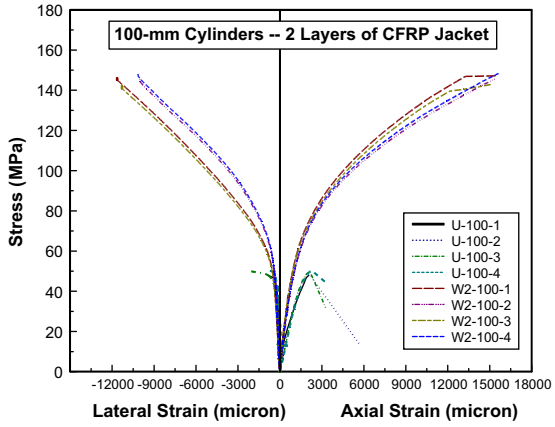

(b) Specimens with 2 layers of CFRP jacket

Fig. 5. Stress–strain curves for 100-mm cylinders.

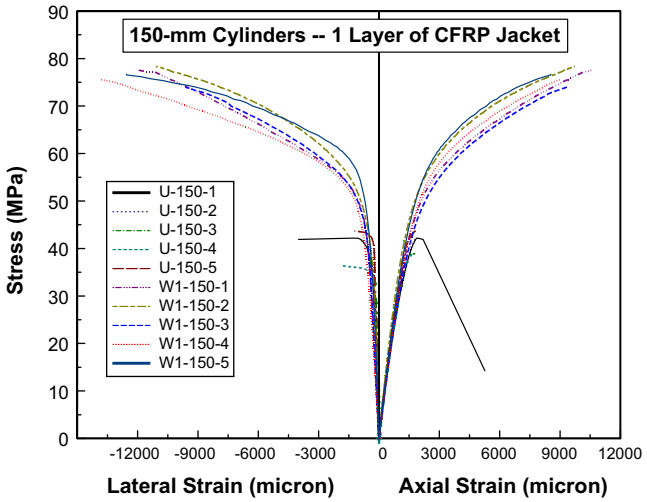

(a) Specimens with 1 layer of CFRP jacket

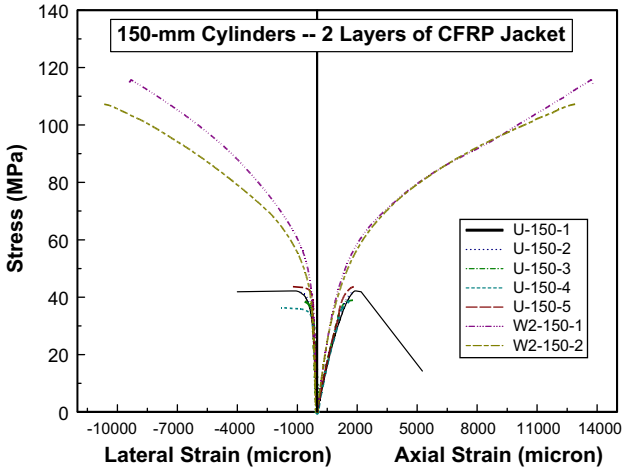

(b) Specimens with 2 layers of CFRP jacket

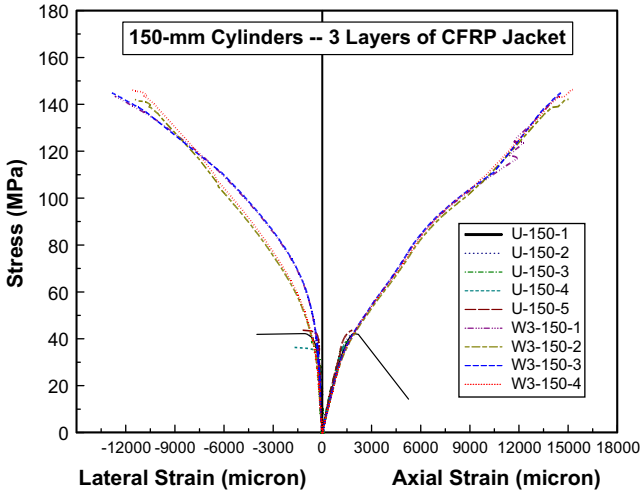

(c) Specimens with 3 layers of CFRP jacket

Fig. 6. Stress–strain curves for 150-mm cylinders.

A review of existing literature produced very few studies on the topic of size effect on FRP-confined concrete. As there is currently a great interest in developing design guidelines for FRP-strengthened concrete columns, it is important to ensure that the proposed equations in literature are truly representative of the actual behavior of full-scale columns. Since most of the available data regarding FRP-confined concrete has been generated from tests on small-scale cylinders, the validation of these results and their applicability to large-scale columns is of great practical interest. This study focuses on various aspects of the effects of the size of FRP-confined concrete cylinders. Using the same concrete mix, size effects are investigated through tests on specimens having three different diameters having the same slenderness ratio (H/D). A total of 37 concrete specimens

Table 4
Specimens used in the finite element analysis.

Specimen designation	Diameter, D (mm)	Height, H (mm)	No. of CFRP layers	Thickness of CFRP jacket, t_j (mm)	Confinement ratio ($\rho_i = 4t_i/D$)
U-50	50	100	–	–	0
U-100	100	200	–	–	0
U-150	150	300	–	–	0
W0.333-50	50	100	0.333	0.333	0.027
W0.5-50	50	100	0.5	0.5	0.04
W0.667-50	50	100	0.667	0.667	0.053
W1-50	50	100	1	1	0.08
W0.667-100	100	200	0.667	0.667	0.027
W1-100	100	200	1	1	0.04
W1.333-100	100	200	1.333	1.333	0.053
W2-100	100	200	2	2	0.08
W1-150	150	300	1	1	0.027
W1.5-150	150	300	1.5	1.5	0.04
W2-150	150	300	2	2	0.053
W3-150	150	300	3	3	0.08
W6-900	900	1800	6	6	0.027
W9-900	900	1800	9	9	0.04
W12-900	900	1800	12	12	0.053
W18-900	900	1800	18	18	0.08

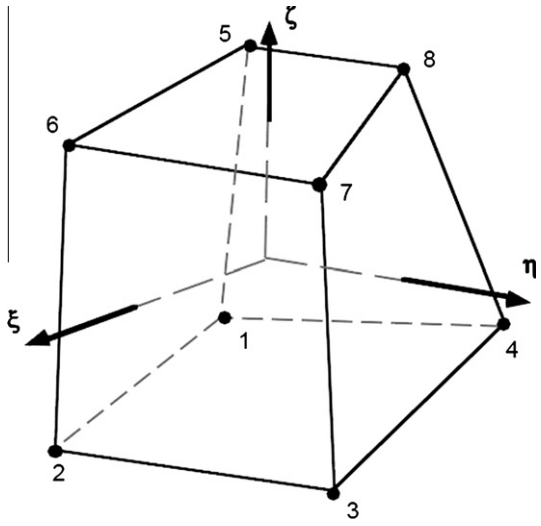

Fig. 7. Eight node solid hexahedron element.

Table 5
Details of finite element mesh.

Specimen diameter	Size of elements	No. of elements
50 mm	3–6 mm	768 shells 3456 solids
100 mm	6–11 mm	768 shells 3456 solids
150 mm	9–16 mm	768 shells 3456 solids
900 mm	28–50 mm	3072 shells 26,112 solids

were tested under uniform uniaxial compression. The data recorded included compressive loads in addition to axial and lateral strains. Non-linear finite element (FE) modeling of FRP-confined concrete was carried out using the program LS-DYNA [16]. Results obtained from the numerical modeling were compared with the experimental results of the specimens tested in this study in addition to others selected from the literature. Using the validated model, the effect of specimen size taking into account various confinement ratios, on

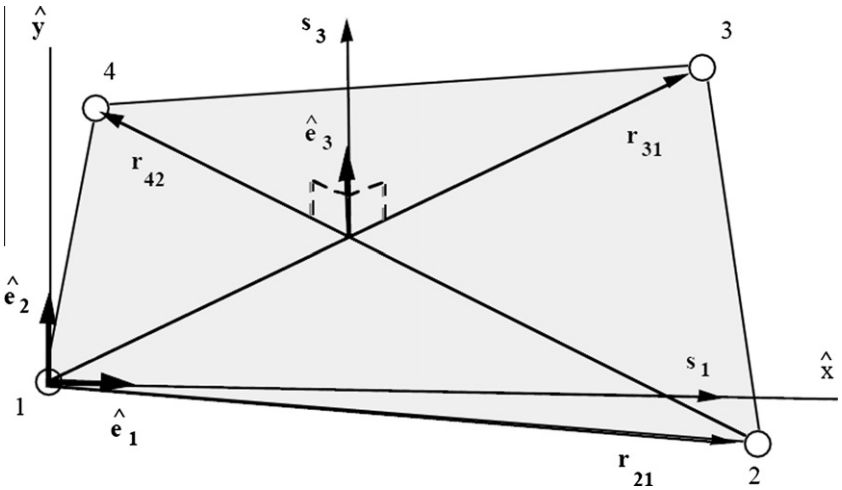

Fig. 8. Shell element co-ordinate system.

the confined concrete, was then numerically studied. Although there have been well documented experimental and analytical studies referring to the non-linear modeling of FRP-confined concrete, most of the models have more of a theoretical significance rather than a practical approach [17,18]. This study also aims to develop and validate a non-linear FE model based on material models existing in the LS-DYNA program database which would be successful in simulating the response of concrete confined with FRP jackets, to further understand its stress–strain behavior and failure mechanisms. The model should therefore be of significance for practical implications.

2. Experimental program

2.1. Test matrix

Details of the test matrix are listed in Table 1. As indicated, three different sizes of cylinders have been used. Test specimens have been designated using four character naming codes. The first letter U and W indicates control and wrapped specimens, respectively. The first number in the designation denotes the number of CFRP layers. The next number indicates the diameter (in mm) of test specimens; whereas, the last is for the specimen number. As an example, Specimen: W2-100-3 denotes a 100 mm diameter specimen wrapped with two layers of CFRP jacket. The last character in the code signifies that it would be the third specimen of this type. The absence of this character means that average value of all the specimens has been considered.

2.2. Preparation of specimens

For the concrete mix used in this study, the average compressive strength of the standard 150-mm cylinders was 41.1 MPa. The quantities of ingredients used in the concrete mix are shown in Table 2. A total of 37 plain concrete cylinders with three different cross-sectional sizes (50×100 mm, 100×200 mm and 150×300 mm) were cast. After 28 days of curing, before wrapping the specimens, they were sandblasted and voids and deformities on the surface of the specimens were filled using gypsum paste. The two part epoxy system used was thoroughly hand-mixed for at least 5 min before use. The CFRP laminates were then applied directly onto the surface of the specimens providing unidirectional lateral confinement in the hoop direction. Special care was taken by the installers to eliminate any voids between the FRP laminates and the concrete substrate. All wrapped specimens were stored at room temperature for at least 7 days before testing in order to ensure that enough time had passed for the epoxy to cure. Prior to loading the specimens on to the test machine, the ends of the jacket were ground smoothed to remove any uneven edges. Representative samples of control and wrapped cylinders are shown in Fig. 1.

2.3. Instrumentation and test procedure

All cylinders were capped with sulfur to ensure parallel surface and to distribute the load uniformly in order to reduce eccentricity. All specimens were instrumented by two horizontal strain gages

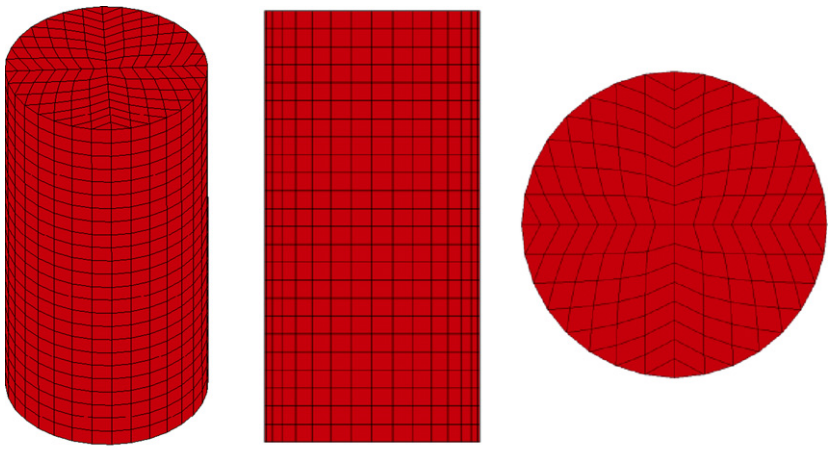

(a) Concrete volume

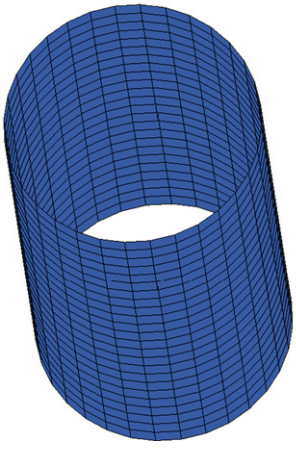

(b) FRP jacket

Fig. 9. Finite element mesh for 50-mm, 100-mm and 150-mm cylinders.

mounted at its mid-height on opposite surfaces of the cylinder, to record the lateral strains during the experiment. In order to measure axial strains, each specimen was fitted with a compressometer which comprised of two LVDTs that were mounted on two round sleeves around the specimen. The sleeves were attached to the specimen with pin-type support that would not affect the dilation of concrete. The testing was performed using 2000-kN hydraulic testing machine equipped with a moving piston that exerts an axial force. Testing was carried out as per the ASTM-standard C39 [11] and was controlled by displacement till failure of cylinders. Layout of instrumentation is presented in Fig. 2.

3. Experimental results

Fig. 3 shows the failed specimens for representative samples of control and wrapped cylinders. For the control specimens, mode of failure can be characterized by shearing and splitting of concrete. The performance of wrapped specimens was consistent. Prior to the failure, cracking noises were heard, indicating the start of stress transfer from the dilated concrete to the CFRP jacket. The failure was gradual and ended with a sudden and explosive noise. It was characterized by the crushing of concrete followed by cutting of the CFRP laminates at the middle portion of the specimen. The jacket rupture started at its mid-height and progressed upwards and downwards. The sudden and explosive nature of the failure indicates the release of tremendous amount of energy as a result of the uniform confining stress provided by the jacket. Inspection of the failed specimens showed good contact between the jacket and the concrete indicating that no debonding took place at any stage throughout the loading process.

Summary of test results is listed in Table 3 as average values for peak axial stress, peak axial strain and peak lateral strain. The table also lists the ratio of average compressive strength of specimens (f'_{cu}), to the average compressive strength of the standard 150-mm cylinder (f'_c) and the ratio of average compressive strength of specimens (f'_{cu}), to the average unconfined compressive strength of the cylinders (f'_{co}). Columns 6 and 7 of the table represent the ratio of the average ultimate compressive strain (ϵ_{cu}) of the specimens to the nominal ultimate strain of unconfined concrete, (ϵ_{co}) taken as 0.003 [19] and the ratio of the average ultimate compressive strain (ϵ_{cu}) to the average ultimate strain of unconfined specimens, (ϵ_{cuu}), respectively.

The experimental results tabulated indicate that, for the case of 50, 100 and 150 mm diameter specimens, wrapped with a single layer of CFRP, the peak axial stress increased by 172%, 92% and 86% respectively. For the case of 100 and 150 mm cylinders wrapped with two layers of CFRP, the percentage increase in the peak axial stress was 197% and 171%, respectively. The 150 mm diameter specimens wrapped with three layers of CFRP experienced a 251% increase in their peak axial stress. It should be noted that the percentages are in comparison with the respective control specimens.

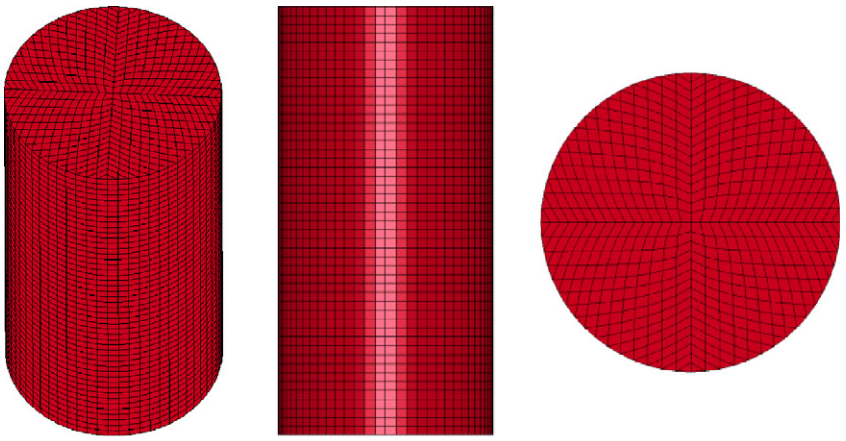

(a) Concrete volume

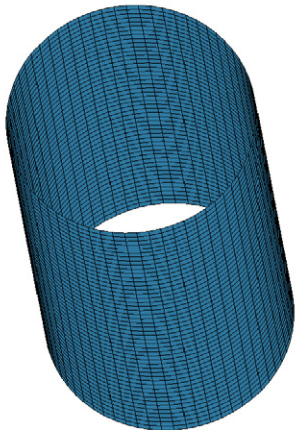

(b) FRP jacket

Fig. 10. Finite element mesh for 900-mm cylinders.

For the case of peak axial strain, compared with the control specimens, it was noticed that, the 50, 100 and 150 mm diameter specimens wrapped with a single layer of CFRP, experienced an increase of 354%, 203% and 161%, respectively. For the case of 100 and 150 mm cylinders wrapped with two layers of CFRP, the percentage increase in the peak axial strain was 327% and 269%, respectively. The 150 mm diameter specimens were the only ones wrapped with three layers of CFRP and they experienced an average increase of 311% in the observed peak axial strain.

Comparison between the peak lateral strain values of the unconfined and confined 50, 100 and 150 mm diameter specimens revealed that for cylinders wrapped with one layer of CFRP, the percentage increase in the peak lateral strain was 696%, 807% and 907%, respectively. The 100 and 150 mm specimens wrapped with two layers of CFRP gained a percentage increase of 847% and 759%, respectively, in the peak lateral strain values. A gain in the peak lateral strain of 937% was recorded in the 150 mm specimens wrapped with three layers of CFRP, compared with the unconfined 150 mm diameter specimens.

A comparison of results for the wrapped specimens of different diameters but having the same confinement ratio of 0.08, (W1-50, W2-100 and W3-150) indicated that the peak axial stress and strain values were very close to each other. The respective peak axial stress values for the abovementioned 50, 100 and 150 mm diameter specimens were 146.2, 146 and 144.2 MPa and the respective peak axial strain values were 15,625, 15,410 and 14,852 micro-strain, as tabulated in Table 3.

Fig. 4 shows the axial stress versus axial strain and lateral strain curves for the all 50 mm diameter, control and singly wrapped specimens. Figs. 5 and 6 show the same curves for 100 and 150 mm diameter specimens, wrapped with 1 and 2 layers and 1, 2 and 3 layers of CFRP, respectively.

4. Finite element modeling

Finite element modeling of the wrapped as well as the control concrete cylinder specimens was carried out in order to validate the finite element modeling and analysis techniques used in this study, with the results obtained from the experimental tests performed. LS-DYNA [16], a general-purpose transient finite element program, was employed for the numerical simulation of the cylinder specimens. This software incorporates a well-tested and validated concrete damage model and a damage model for FRP composites as well. The program has options for analyzing static as well as dynamic response of structures. The selection of this program for the study was also made since a licensed version was readily available on the University servers. The 3-D finite element model was developed using a program FEMB, which is a preprocessor for LS-DYNA.

In addition to the 50, 100 and 150 mm diameter specimens, using the validated numerical techniques described in this section, 900 mm diameter cylinder specimens were also modeled in this study. No experimental results were available for these specimens. Table 4 lists all specimens used in the finite element analysis. As seen in Table 4, for the case of CFRP-wrapped specimens, 4 different confinement ratios viz. 0.027, 0.04, 0.053, 0.08 and cylinder diameters viz. 50, 100, 150, 900 mm, were considered in the numerical analysis to study the size effect.

4.1. Model geometry

In order to mimic the real behavior of concrete cylinders, it is imperative that the concrete volume be modeled using solid elements. For this reason, 8-node reduced integration solid hexahedron elements were used to model the concrete. These elements have three degrees of freedom at each node. Single point volume integration is carried out by Gaussian quadrature. Hourglass control is provided in order to avoid the zero energy modes. Fig. 7 shows the standard 8-node hexahedron solid element geometry.

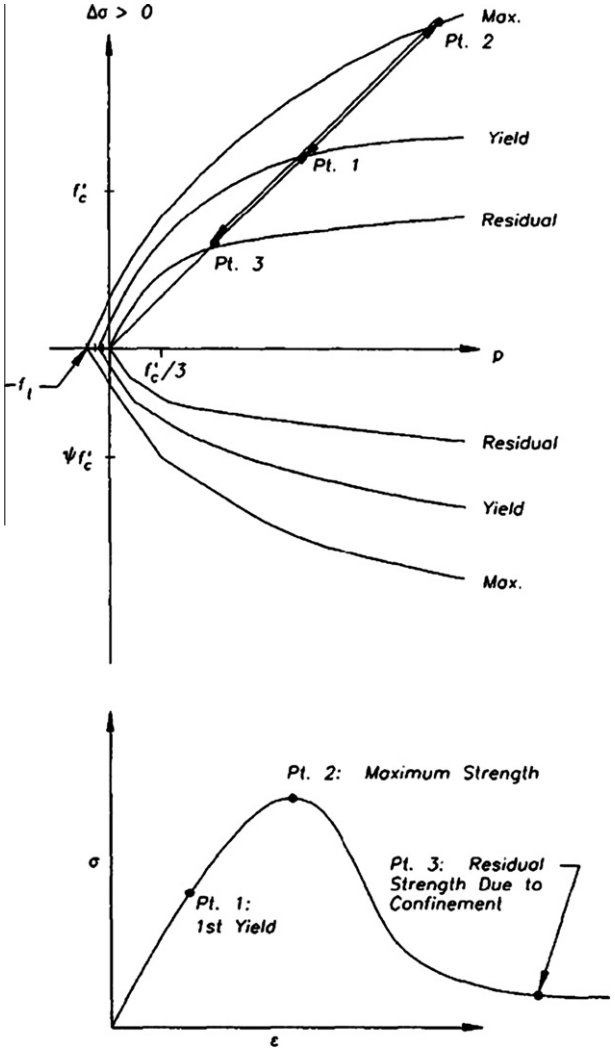

Fig. 11. Concrete damage material model: three failure surfaces.

Table 6
Material properties used in the analysis.

Material model	Type 072R3 (Karagozian & case model)
Concrete	
Uni-axial compressive strength (MPa)	41.1
Density (kg/m^3)	2170
Poisson's ratio	0.2
	Type-022 (composite damage model)
CFRP[*]	
Thickness of each layer (mm)	1.0
Young's modulus in long. dir. (MPa)	77,300
Young's modulus in transverse dir. (MPa)	3380
Longitudinal tensile strength (MPa)	846
Transverse tensile strength (MPa)	40.6

[*] Results obtained from testing standard composite coupons in the lab.

FRP jackets were modeled using 4-node shell elements with 6 degrees of freedom at each node. These elements include membrane, bending and shear deformation capabilities. The section attribute for this element is thickness alone. The Belytschko–Tsay [20] element formulation was used for the shell elements, which is also the default theory for shell elements in LS-DYNA as a result of its computational efficiency. It is based on a combined co-rotational and velocity strain formulation. The co-rotational portion of the formulation avoids the complexities of non-linear mechanics by embedding a co-ordinate system in the element. Fig. 8 describes the construction of element co-ordinate system for the shell elements used. Full bond was assumed between the FRP jacket and the concrete substrate. An optimum mesh size was chosen for model components, which is described in Table 5 for the different sizes of cylindrical specimens. Fig. 9 depicts the mesh geometry used in this study for 50, 100 and 150 mm diameter specimens;

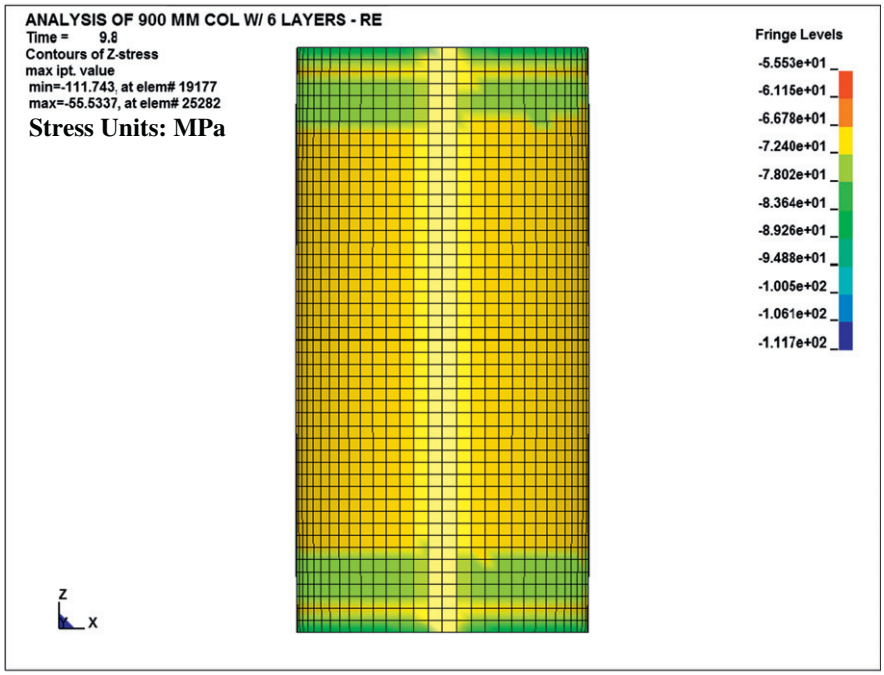

(a) Contours of axial stress in concrete volume at ultimate condition

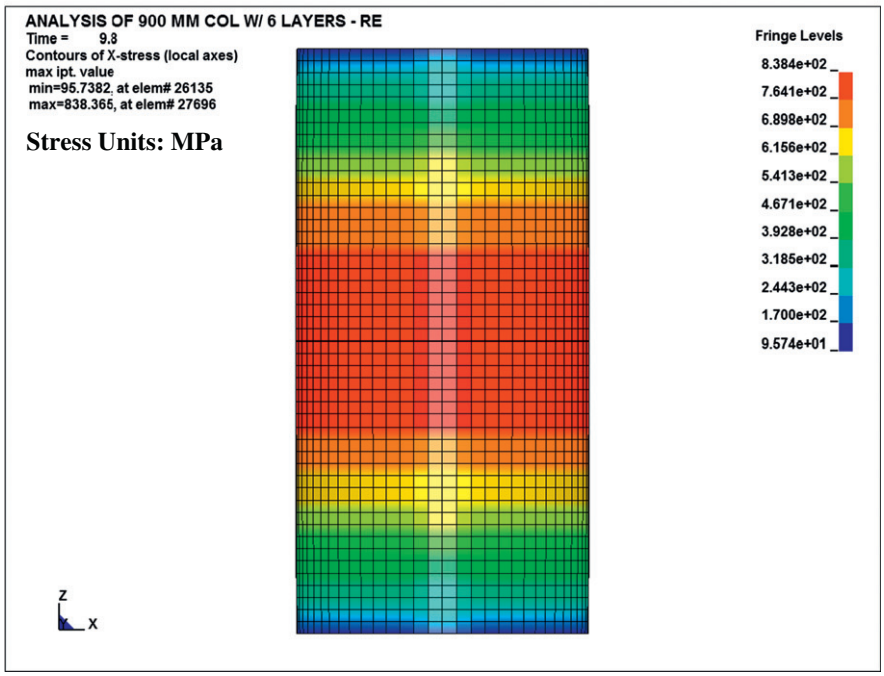

(b) Contours of hoop stress in FRP jacket at ultimate condition- max hoop stress = 838 MPa

Fig. 12. Stress contours in 900-mm specimen with six layers of CFRP at ultimate condition.

whereas, Fig. 10 displays the mesh used for 900 mm specimens. It has been proven in this study that further decrease in the mesh size beyond that listed in Table 5 and shown in Figs. 9 and 10 has insignificant effect on the numerical results but leads to the risk of computer memory overflow and substantially increases the computing time.

4.2. Material modeling

LS-DYNA program incorporates material cards to define the materials used for the analysis. In this study, concrete was modeled using the Karagozian and Case (K&C) [21], concrete model "CONCRETE_DAMAGE_RELEASE 3", which is a three invariant

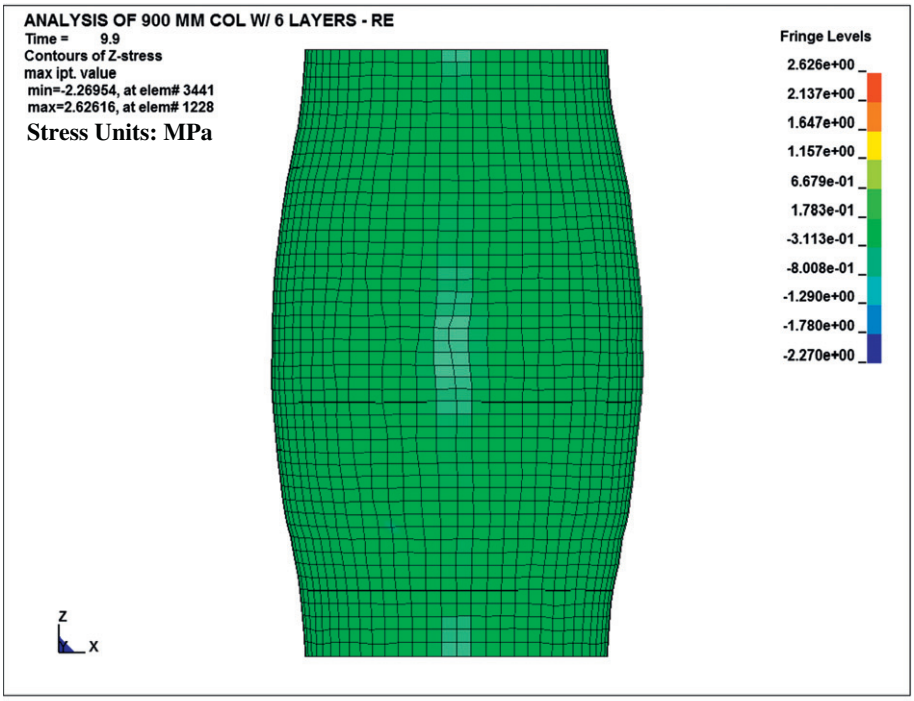

(a) Contours of axial stress in concrete volume at jacket fracture

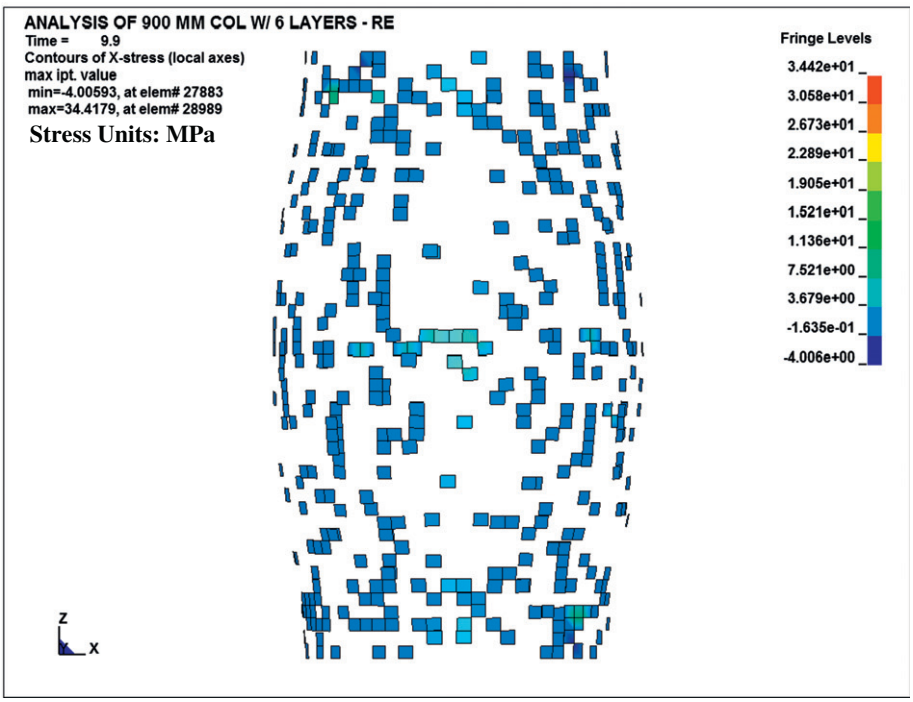

(b) Contours of hoop stress in FRP jacket upon its fracture

Fig. 13. Stress contours in 900-mm specimen with six layers of CFRP at jacket fracture.

model and uses three shear failure surfaces: the initial yield surface, the maximum yield surface, and the residual yield surface as seen in Fig. 11. The model also includes damage and strain rate effects. This model has the capability of model parameter generation based solely on the unconfined compressive strength of concrete. It also incorporates many important features of concrete behavior such as tensile fracture energy, shear dilation and effects of confinement. During initial loading, the deviatoric stresses are elastic until the initial yield surface is reached. Then, the stresses can increase further until they reach the maximum yield surface. Beyond the maximum yield surface, the response can soften to the residual surface or be perfectly plastic [22]. The material card has the option of inputting various material parameters such as concrete density, Poisson's ratio, compressive strength of concrete, aggregate size, etc. It should be noted that for FRP-wrapped specimens, the compressive strength input for the concrete model was the unconfined compressive strength of concrete.

The CFRP laminates were modeled using the material model type MAT_022, MAT_COMPOSITE_DAMAGE, which can be used to define arbitrary orthotropic materials such as unidirectional layers in composite shell structures. The laminated shell theory was used for the purpose of correcting the assumption of a uniform constant shear strain throughout the thickness of the composite shell, thus avoiding very stiff results. The PART_COMPOSITE card was used to define a part which simplifies the method of defining a composite material for shell elements by eliminating the need for user defined integration rules and part Id's for each layer of the composite material. It also allows the input of material ID, composite thickness and material orientation for each of the composite layers. Table 6 shows some of the material properties input in the material cards of the LS-DYNA program.

4.3. Boundary conditions and loading strategy

In order to simulate the displacement boundary condition of the base of the cylinder, a node set was created which consisted of the nodes corresponding to the volume of concrete cylinder in contact with the surface below. For this set of nodes, the nodal constraints were applied for translation in the global X, Y and Z directions. Another node set was created for the nodes corresponding to the volume of cylinder which is in contact with the loading (top surface). For this set, nodal constraints were applied for translation in the global X and Y directions, whereas the nodes were free to translate in the z-direction. LS-DYNA uses explicit time integration algorithms for solving the problems, which are less sensitive to machine precision than other finite element solution methods. The load application process in LS-DYNA is time-history dependent. The program provides a way of defining imposed motions on boundary nodes. For this purpose, the BOUNDARY_PRESCRIBED_MOTION card was used to apply imposed nodal motion to the set of nodes along the loading plane. However, since the testing procedure involved displacement controlled static loading in the axial direction, the inertia effects were removed from the dynamic equation by assigning a constant velocity to the displacement controlled node set. This will lead to zero acceleration and hence zero inertia force. The loading control rate was set to 0.001 mm/mm/sec.

4.4. Modes of failure

Figs. 12 and 13 depict the mode of failure for a representative case of 900-mm specimen with six layers of CFRP jacket as observed from the FE analysis post-processing software. The failure

Table 7
Specimens selected from other studies for validation of FE results.

Specimen designation	Specimen source	Diameter, D (mm)	Height, H (mm)	Compressive strength of concrete, f'_c (MPa)	Properties of FRP jacket			
					Type of fiber	Thickness (mm)	Young's modulus in long. dir. (MPa)	Longitudinal tensile strength (MPa)
W50 – Ref. [23]	Harmon and Slattery [23]	50	100	41	Carbon	0.344	235,000	1763
W100 – Ref. [24]	Al-Salloum et al. [24]	100	200	38.8	E-glass	1.3	27,600	552
W150 – Ref. [25]	Rochette and Labossiere [25]	150	300	43	Aramid	3.86	13,600	230

Table 8
Summary of comparison between experimental and numerical results.

Specimen designation	Peak axial stress (MPa)			Peak axial strain (micro-strain)		
	EXP*	NUM	EXP/NUM	EXP*	NUM	EXP/NUM
Specimens tested in this study						
U-50	53.8	55.9	0.962	3440	2860	1.202
U-100	49.1	49.5	0.991	3605	5800	0.621
U-150	41.1	42.8	0.960	3616	5900	0.612
U-900	–	35.2	–	–	4000	–
W1-50	146.2	155.8	0.938	15,625	18,400	0.849
W1-100	94.5	95.8	0.986	10,907	11,700	0.932
W2-100	146.0	153.1	0.953	15,410	18,200	0.846
W1-150	76.4	77.4	0.987	9445	9900	0.954
W2-150	111.5	115	0.969	13,353	13,900	0.960
W3-150	144.2	156.5	0.921	14,852	18,100	0.820
Specimens tested by other researchers						
W50-Ref. [23]	158.3	163.7	0.967	NA	12,700	-
W100-Ref. [24]	66.5	70.2	0.947	12,842	13,680	0.939
W150-Ref. [25]	71.0	74.0	0.959	16,900	14,520	1.164

* Average values for specimens.

mode in the figure is based on contours of global *Z*-stress for concrete volume and local *X*-stress (hoop stress) for FRP jacket. From the figures it can be seen that the wrapped specimen failed due to facture of the FRP jacket followed by excessive dilation and crushing of the confined concrete core.

4.5. Validation of finite element analysis

The validation of the FE analysis and the modeling techniques was carried out by comparing the results of the experimental tests implemented in the current study and some selected studies by other researchers [23–25], with the numerical results obtained from the FE model prepared in this research. Table 7 presents the details of the specimens, including their designation, which were selected from other studies for the purpose of validation.

The comparison between experimental results from the current study and the FE results was made by generating axial stress–strain curves for the 50, 100 and 150 mm cylinders for both unconfined and confined specimens. Table 8 presents a summary of results showing the comparisons between the experimental and numerical results. Figs. 14–16 show the axial stress versus strain curves for the unconfined specimens of diameter 50, 100 and 150 mm, respectively. The curves consist of test results obtained from experimental testing as well as the predicted response curve of the FE model developed in this study. From the figures it can be seen that the predicted response of the FE model was generally in close agreement with the experimental results, especially in terms of predicted peak strength of unconfined concrete. Figs. 17–19 depict the stress–strain comparison curves of the CFRP-confined concrete cylinder specimens with diameters of 50, 100 and 150 mm, respectively. As seen in Figs. 17–19, the predicted response of the FE model agree quite well with the test results.

However, for the results obtained from other studies, a comparison was made, only between the peak axial stress and axial strain values in the absence of the full stress–strain curves. As seen in Table 8, the experimental to numerical peak axial stress ratios for the three specimen sizes 50, 100 and 150 mm selected from other researchers, were 0.967, 0.947 and 0.959, respectively. For the peak axial strain values, the experimental to numerical ratios were 0.939 and 1.164 for the 100 and 150 mm specimens, respectively. For the 50 mm specimen, the experimental value of the peak axial strain was not reported in the study.

Based on this comparison, it is clear that the compressive strength of FRP-confined concrete was predicted excellently by the model developed in this study. The results for specimens considered for numerical analysis only, are listed in Table 9.

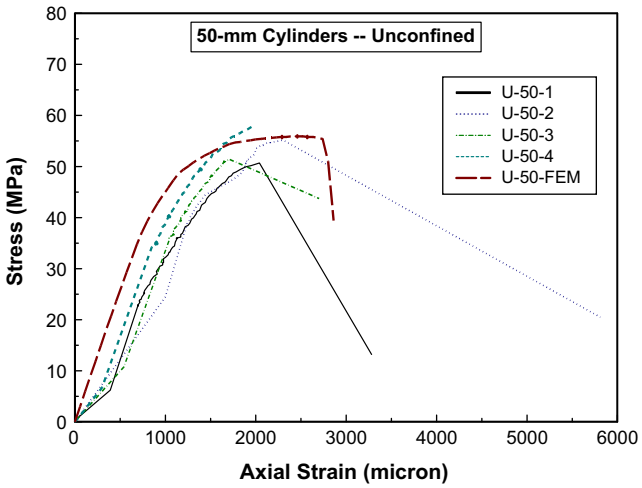

Fig. 14. Stress–strain comparison for control 50-mm cylinders.

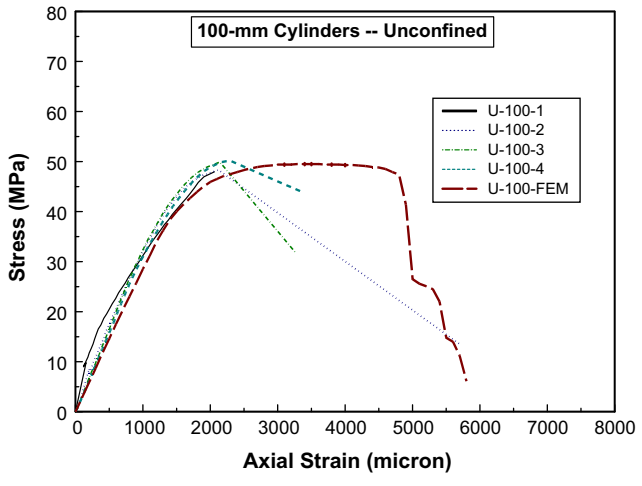

Fig. 15. Stress–strain comparison for control 100-mm cylinders.

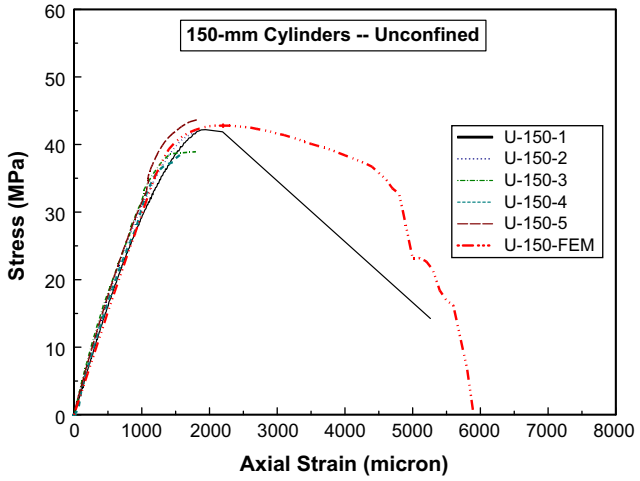

Fig. 16. Stress–strain comparison for control 150-mm cylinders.

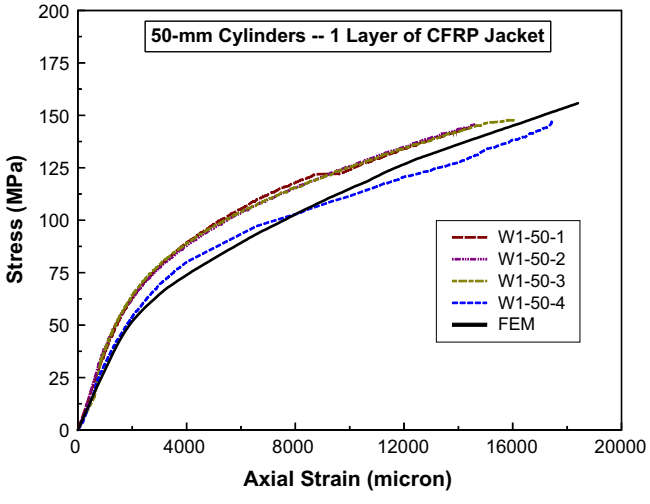

Fig. 17. Stress–strain comparison for CFRP-wrapped 50-mm cylinders.

5. Discussion

5.1. Effect of specimen size

5.1.1. Based on experimental results

In order to study the effect of specimen size on the ultimate strength of unconfined concrete, the relationship between specimen diameter and strength ratio (ratio of compressive strength, f'_{cu}, to compressive strength of standard 150-mm cylinder, f'_c) for the experimental specimens was generated as displayed in Fig. 20a. From the figure, it is clear that the size effect is pronounced for unconfined concrete. However, the same is not true for CFRP-confined specimens. For the case of wrapped specimens, the effect of specimen size was studied based on comparison of results obtained for specimens having the same confinement ratio of 0.08 (W1-50, W2-100 and W3-150). Fig. 20b presents the relation between specimen diameter and strength enhancement ratio (ratio of confined concrete strength, f'_{cu} to unconfined compressive strength of standard 150-mm cylinder, f'_c) for specimens with the same confinement ratio of 0.08. In addition, Fig. 20c displays the relation between cylinder diameter and strain enhancement ratio (ratio between ultimate compressive strain of confined concrete, (ϵ_{cu}) and nominal ultimate strain of unconfined concrete, (ϵ_{co}) taken as 0.003 [19]) for specimens with the same confinement ratio of 0.08. From the figures, it is clear that size effect is insignificant on both the strength and strain enhancement of

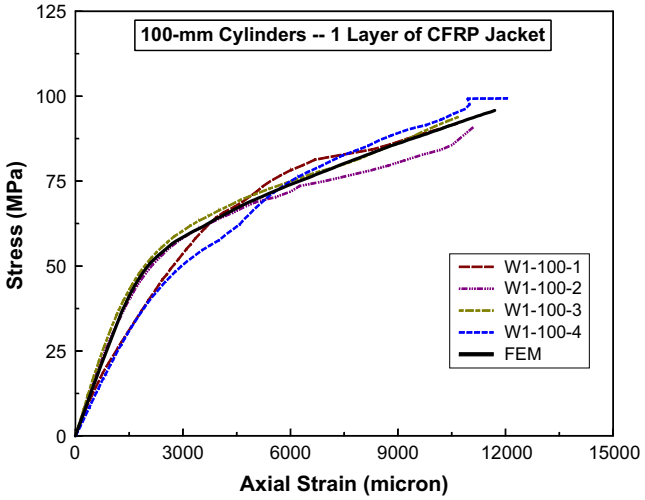

(a) Specimens with 1 layer of CFRP jacket

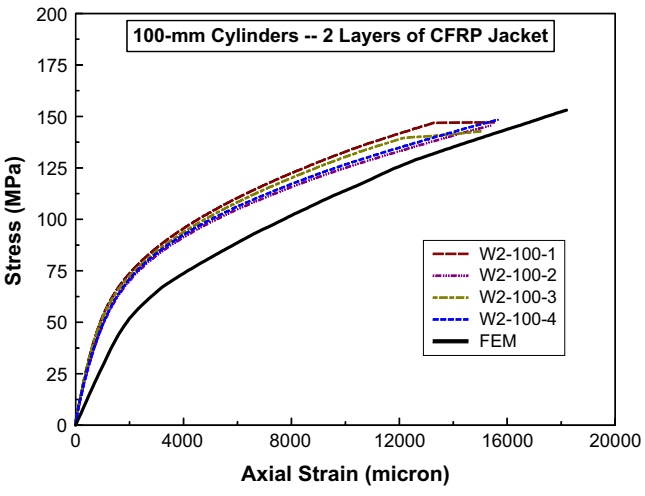

(b) Specimens with 2 layers of CFRP jacket

Fig. 18. Stress–strain comparison for CFRP-wrapped 100-mm cylinders.

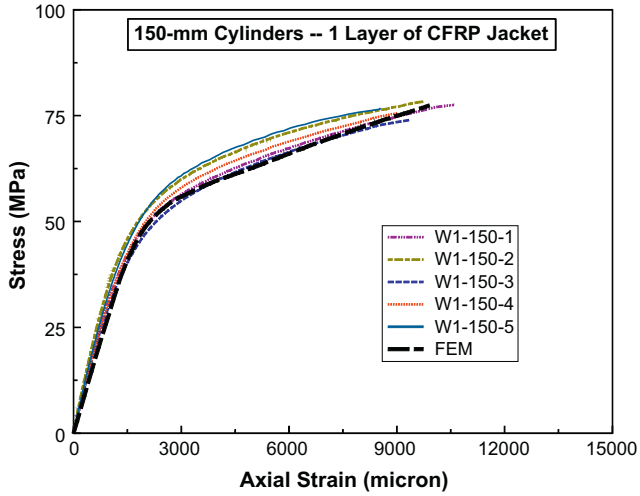

(a) Specimens with 1 layer of CFRP jacket

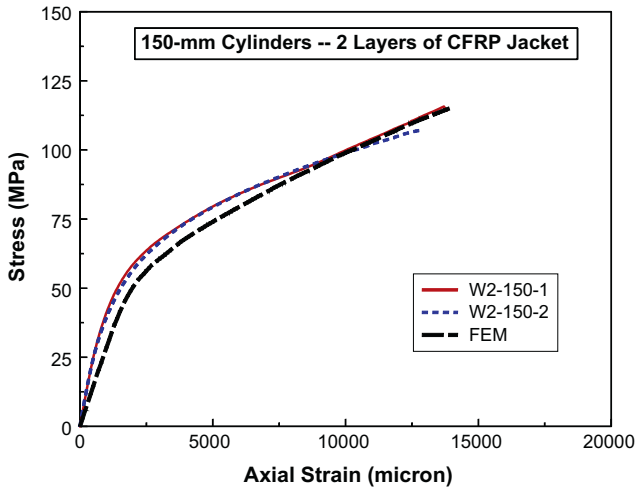

(b) Specimens with 2 layers of CFRP jacket

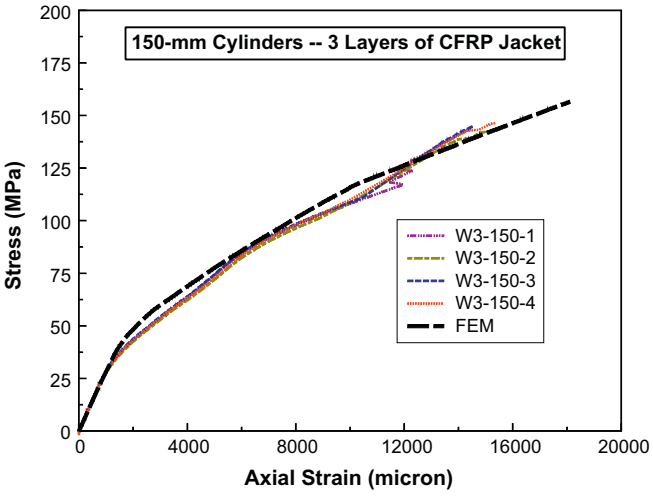

(c) Specimens with 3 layers of CFRP jacket

Fig. 19. Stress–strain comparison for CFRP-wrapped 150-mm cylinders.

FRP-confined concrete for all specimen sizes used in this study. This assessment is in agreement with an earlier study [14] for medium and large size FRP-confined specimens. It should be noted that the results from the smaller diameter specimens (50 mm) were also found to be reliable in this study. Accordingly, there is no need to introduce a size factor for the test results which are based on non-standard sizes of cylindrical specimens before using them in developing analytical models for FRP-confined concrete.

5.1.2. Based on finite element results

Fig. 21 shows the predicted axial stress–strain curves for the different diameter unconfined cylinder specimens, obtained from the validated FE models. As seen in the figure, 900 mm diameter specimen was also included in the results. The effect of size on the peak unconfined concrete strength is clearly evident in the figure.

In order to study numerically the effect of specimen size on CFRP-wrapped cylinders, stress–strain curves were plotted for specimens based on four different confinement ratios viz. 0.027, 0.04, 0.053 and 0.08. Fig. 22 shows the axial stress–strain curves predicted by the validated FE model for the abovementioned confinement ratios and cylinder sizes of 50, 100, 150 and 900 mm. Based on the stress–strain plots obtained from the FE analysis and for the confinement ratios used in this study, it is apparent that the effect of size in FRP-confined concrete is insignificant.

Fig. 23a shows the relationship between specimen diameter and strength ratio (ratio of compressive strength f'_{cu} to compressive strength of standard 150-mm cylinder f'_c) for the unconfined concrete specimens based on the FE model results. The figure shows a distinct effect of specimen size on the peak unconfined concrete strength results. Comparing Figs. 20 and 23a, it can be observed that, the effect of specimen size in unconfined specimens is more pronounced as the specimen size increases from 50 mm up to the 150 mm compared with the increase from 150 mm to the 900 mm specimens. Based on the numerical results, Figs. 23b and 23c depict the relation between specimen diameter and strength enhancement ratio, and the relation between cylinder diameter and strain enhancement ratio, respectively, for CFRP-wrapped specimen. It is evident that the size effect does not play a significant role on both the strength and strain enhancement of FRP-confined concrete.

5.2. Effect of confinement stress ratio

Due to the insignificant effect of specimen size on strength of FRP-confined concrete, all recorded data for FRP-confined specimens used in this study can be mixed together to study the effect of confinement stress ratio (ratio of confinement stress f_l provided by FRP jacket to unconfined compressive strength of standard 150-mm cylinder, f'_c) on both strength and strain enhancement as shown in Figs. 24a and b, respectively. Here, the confinement stress is given as $f_l = 0.5\rho_j f_{ju}$, where ρ_j is the confinement ratio, and f_{ju} is the longitudinal tensile strength of the FRP material. It is evident

Table 9
Numerical results for specimens without experimental data.

Specimen designation	Peak axial stress (MPa)	Peak axial strain (micro-strain)
U-900	35.2	4000
W0.333-50	78.8	9900
W0.5-50	97.7	11,800
W0.667-50	117.8	14,100
W0.667-100	77.7	9900
W1.333-100	115.5	13,900
W1.5-150	95.4	11,700
W6-900	74.2	9800
W9-900	93.1	11,700
W12-900	114.9	13,700
W18-900	149.9	18,200

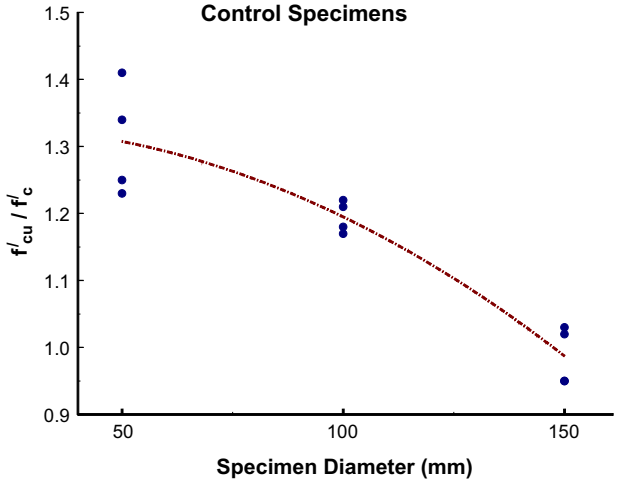

(a) Control specimens –ultimate strength ratio

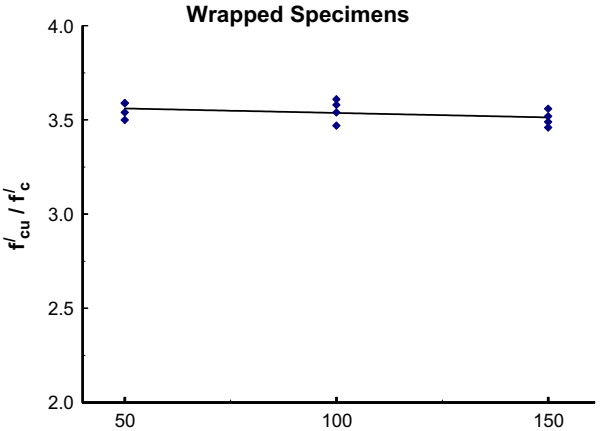

(b) Wrapped –strength enhancement

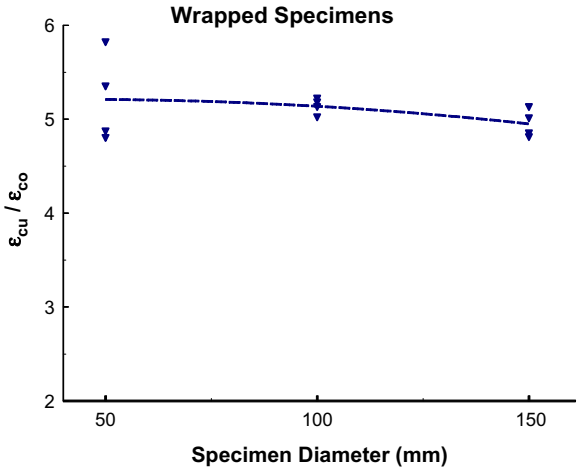

(c) Wrapped –strain enhancement

Fig. 20. Effect of specimen size on strength and strain enhancement: experimental results.

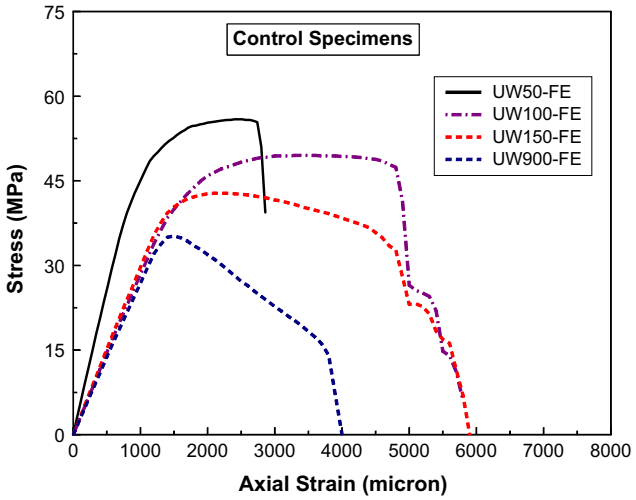

Fig. 21. Effect of specimen size on stress–strain curve for control specimens – finite element results.

that as the confinement stress ratio increases the gain in strength and ductility increases for FRP-confined concrete. Based on the results obtained from 24 CFRP-wrapped cylinders tested in this study, a linear regression analysis was carried out in order to correlate the confinement stress ratio with the strength and strain enhancement ratios, and the following regression models are proposed. The coefficients of determination (R^2) for the strength and strain regression models proposed in this study were 0.99 and 0.91, respectively.

$$\text{For strength enhancement}: f_{cu}/f'_c = 1 + 3 * (f_l/f'_c) \quad (1)$$

$$\text{For strain enhancement}: \epsilon_{cu}/\epsilon_{co} = 2.14 + 3.65 * (f_l/f'_c) \quad (2)$$

6. Conclusions

The objective of this experimental program and the accompanying finite element analysis was to determine the effect of specimen diameter size, provided the slenderness ratio (H/D) is constant, on increase in strength and ductility under axial compression achieved by wrapping concrete cylinders with FRP. The following conclusions can be made from this study.

(1) Similar to all other previous research, it is evident that the size effect is pronounced for unconfined concrete.
(2) From the experimental and numerical investigations of size effects in FRP-wrapped concrete cylinders, it is concluded that with the same confinement ratio, no significant variations occur in both compressive strength and ultimate strain when different sizes of FRP-confined concrete cylinders were used. Accordingly, there is no need to introduce a size factor for the test results which are based on non-standard sizes of cylindrical specimens before using them in developing analytical models for FRP-confined concrete.

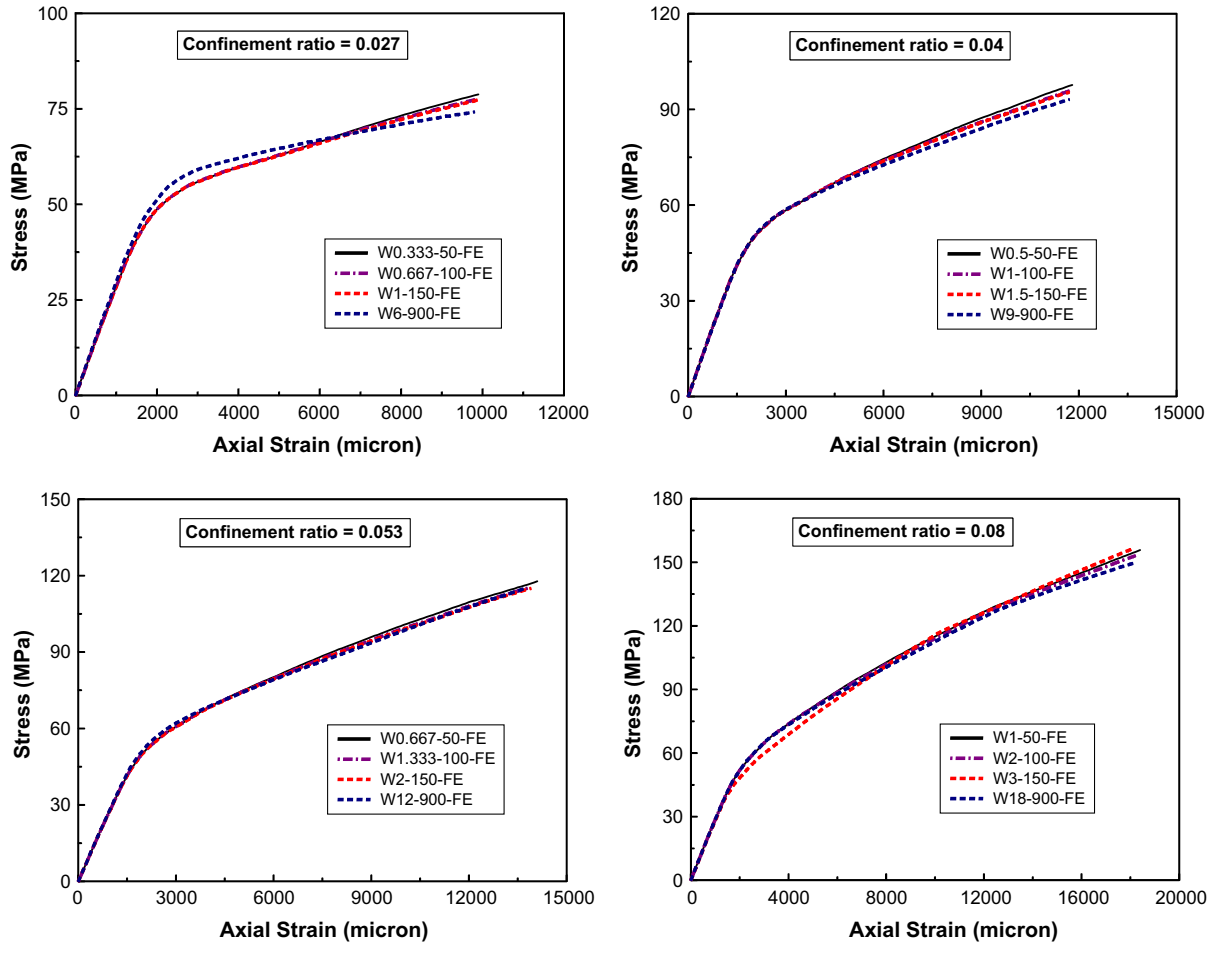

Fig. 22. Effect of specimen size on stress–strain curve for wrapped specimens – finite element results.

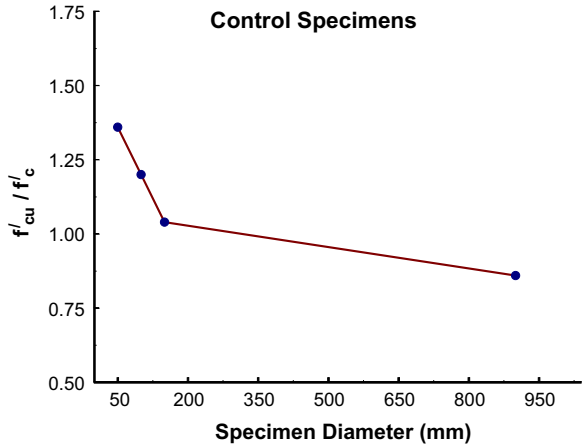

(a) Control –ultimate strength ratio

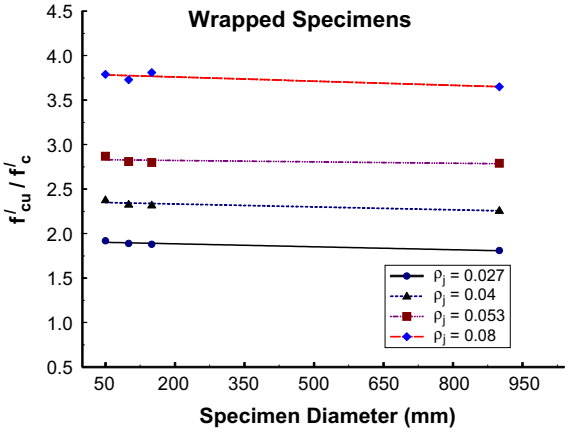

(b) Wrapped –strength enhancement

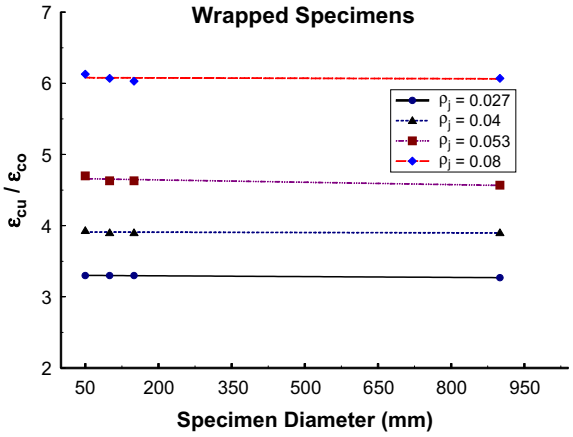

(c) Wrapped –strain enhancement

Fig. 23. Effect of specimen size on strength and strain enhancement – finite element results.

(3) Comparison of the finite element analysis results with the experimental results confirmed that the proposed numerical approach is appropriate for estimating the peak axial compressive strength and the stress–strain behavior of both the unconfined and FRP-confined concrete specimens. This will thereby indicate the validity of the numerical modeling procedures, which may be used for conducting future research in the area of FRP-confined concrete.

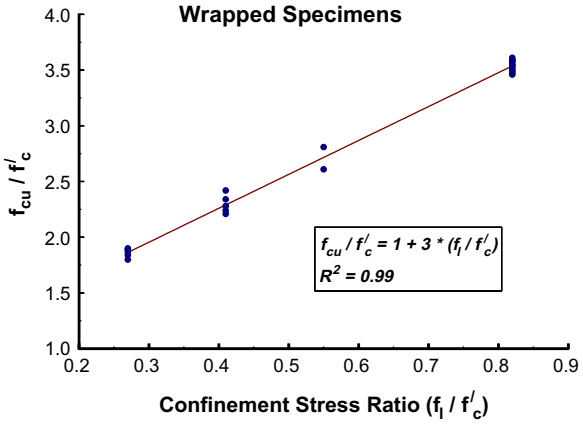

(a) Strength enhancement

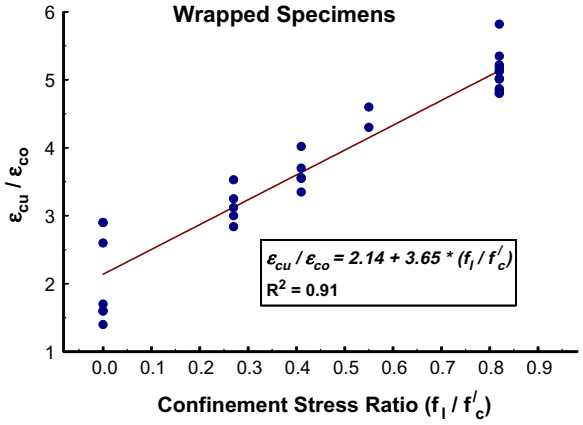

(b) Strain enhancement

Fig. 24. Effect of confinement stress ratio on strength and strain enhancement.

(4) Based on the experimental and finite element results, it is evident that for FRP-wrapped specimens as the confinement stress ratio increases the gain in strength and ductility also increases.

Acknowledgements

The authors gratefully acknowledge the support provided by the Specialty Units for Safety and Preservation of Structures and the MMB Chair of Research and Studies in Strengthening and Rehabilitation of Structures at Civil Engineering Department, King Saud University, Riyadh.

References

[1] Al-Salloum YA. A general model for compressive strength of FRP-confined concrete. In: Proceedings of the 4th international conference on FRP composites in civil engineering (CICE2008), Zürich, Switzerland; 2008.
[2] Demers M, Neale KW. Confinement of reinforced concrete columns with FRP composite sheets – an experimental study. Can J Civ Eng 1999;26:226–41.
[3] Haroun MA, Elsanadedy HM. Fiber-reinforced plastic jackets for ductility enhancement of reinforced concrete bridge columns with poor lap-splice detailing. J Bridge Eng, ASCE 2005;10:749–57.
[4] Saafi M, Toutanji HA, Li Z. Behavior of concrete columns confined with fiber reinforced polymer tubes. ACI Mater J 1999;96(4):500–9.
[5] Toutanji H, Balagurce P. Durability characteristics of concrete columns wrapped with FRP tow sheets. J Mater Civ Eng 1998:52–7.
[6] Parvin A, Jamwal AS. Effects of wrap thickness and ply configuration on composite-confined concrete cylinders. J Compos Struct 2005;67(4):437–42.
[7] Berthet JF, Ferrier E, Hamelin P. Compressive behavior of concrete externally confined by composite jackets. Part A: experimental study. Construct Build Mater 2005;19(3):223–32.

[8] Lam L, Teng JG. Design-oriented stress–strain model for FRP confined concrete. Construct Build Mater 2003;17(6–7):471–89.
[9] Almusallam TH. Behavior of normal and high-strength concrete cylinders confined with E-glass/epoxy composite laminates. J Compos: Part B 2007;38:629–39.
[10] Youssef MN, Feng MQ, Mosallam AS. Stress–strain model for concrete confined by FRP composites. J Compos: Part B 2007;38:614–28.
[11] ASTM C39/C39M – 10 Standard test method for compressive strength of cylindrical concrete specimens. ASTM; 2010.
[12] Neville AM. Properties of concrete. Essex UK: Longman Group Limited; 1995.
[13] Sener S, Barr BIG, Abusiaf HF. Size effect in axially loaded reinforced concrete columns. J Struct Eng 2004;130:662–70.
[14] Theriault M, Neale KW, Claude S. Fiber-reinforced polymer-confined circular concrete columns: investigation of size and slenderness effects. J Compos Constr 2004;8:313–23.
[15] Masia MJ, Gale TN, Shrive NG. Size effects in axially loaded square-section concrete prisms strengthened using carbon fiber reinforced polymer wrapping. Can J Civ Eng 2004;31:1–13.
[16] LS-DYNA User's Keyword Manual, vol. 1. Version 971. Livermore Software Technology Corporation (LSTC); 2007.
[17] Rouger VC, Luccioni BM. Numerical assessment of FRP retrofitting systems for reinforced concrete elements. J Eng Struct 2007;29:1664–75.
[18] Kwon MH. Three dimensional finite element analysis of reinforced concrete members. PhD thesis. USA: Department of Civil, Environmental, and Architectural Engineering, University of Colorado; 2000.
[19] ACI 318-08. Building code requirements for structural concrete and commentary. Detroit, Mich.: American Concrete Institute; 2008.
[20] Belytschko TB, Tsay CS. Explicit algorithms for non-linear dynamics of shells. AMD, ASME 1981;48:209–31.
[21] Malvar LJ, Crawford JE, Morrill KB. K&C concrete material model Release III – Automated generation of material input. K&C Technical report TR-99-24-B1; 2000.
[22] Malvar LJ, Crawford JE, Wesevich JW, Simons D. A plasticity concrete material model for DYNA 3D. Int J Impact Eng 1997;19(9/10):847–73.
[23] Harmon TG, Slattery KT. Advanced composite confinement of concrete. In: Neale KW, Labossiere P, editors. Proceedings of the first international conference on advanced composite materials in bridge and structures. Sherbocke, Canada: Canadian Society for Civil Engineering; 1992. p. 299–306.
[24] Al-Salloum YA, Elsanadedy HM, Abadel AA. Behavior of FRP-confined concrete after high temperature exposure. Constr Build Mater 2011;25(2):838–50.
[25] Rochette P, Labossiere P. Axial testing of rectangular column models confined with composites. J Compos Constr, ASCE 2000;4(3):129–36.